



Peptidases released by necrotic cells control CD8⁺ T cell cross-priming

Jaba Gamrekelashvili,^{1,2} Tamar Kapanadze,^{1,2} Miaojun Han,¹ Josef Wissing,³ Chi Ma,¹ Lothar Jaensch,³ Michael P. Manns,² Todd Armstrong,⁴ Elizabeth Jaffee,⁴ Ayla O. White,⁵ Deborah E. Citrin,⁵ Firouzeh Korangy,¹ and Tim F. Greten¹

¹Gastrointestinal Malignancy Section, Medical Oncology Branch, National Cancer Institute, NIH, Bethesda, Maryland, USA.

²Department of Gastroenterology, Hepatology and Endocrinology, Medizinische Hochschule Hannover, Hannover, Germany.

³Department of Molecular Structural Biology, Helmholtz-Zentrum für Infektionsforschung, Braunschweig, Germany.

⁴Sidney Kimmel Cancer Center at Johns Hopkins, Johns Hopkins University School of Medicine, Baltimore, Maryland, USA.

⁵Radiation Oncology Branch, National Cancer Institute, Mark O. Hatfield Clinical Research Center, NIH, Bethesda, Maryland, USA.

Cross-priming of CD8⁺ T cells and generation of effector immune responses is pivotal for tumor immunity as well as for successful anticancer vaccination and therapy. Dead and dying cells produce signals that can influence Ag processing and presentation; however, there is conflicting evidence regarding the immunogenicity of necrotic cell death. We used a mouse model of sterile necrosis, in which mice were injected with sterile primary necrotic cells, to investigate a role of these cells in priming of CD8⁺ T cells. We discovered a molecular mechanism operating in Ag donor cells that regulates cross-priming of CD8⁺ T cells during primary sterile necrosis and thereby controls adaptive immune responses. We found that the cellular peptidases dipeptidyl peptidase 3 (DPP-3) and thimet oligopeptidase 1 (TOP-1), both of which are present in nonimmunogenic necrotic cells, eliminated proteasomal degradation products and blocked Ag cross-presentation. While sterile necrotic tumor cells failed to induce CD8⁺ T cell responses, their nonimmunogenicity could be reversed in vitro and in vivo by inactivation of DPP-3 and TOP-1. These results indicate that control of cross-priming and thereby immunogenicity of primary sterile necrosis relies on proteasome-dependent oligopeptide generation and functional status of peptidases in Ag donor cells.

Introduction

Cross-priming of CD8⁺ T cells is a pivotal step for induction of Ag-specific immune responses against malignantly transformed or virally infected cells (1–3). At the same time, CD8⁺ T cell priming and generation of adaptive immune responses needs to be tightly regulated by the innate immune system to avoid unwanted activation, which can lead to autoimmune disorders (4–6). Following infection, pathogens provide Ags and pathogen-associated molecular patterns (PAMPs), which are recognized via pattern recognition receptors (PRRs) expressed by professional APCs, such as DCs, and which trigger adaptive immune responses (5, 7, 8). However, it is not completely clear how dead and dying cells influence processing and presentation of released Ags by DCs in the absence of PAMPs (i.e., under “sterile” conditions) and whether such influence leads to the generation of Ag-specific CD8⁺ T cell responses. Therefore, it is important to understand what defines the immunogenicity of cell death, how Ags can be cross-presented, and what role PAMP analogs play in this process.

According to the danger theory, initially proposed by Matzinger, necrotic cell death is predicted to be dangerous and immunogenic (9). Upon necrosis, cellular integrity is lost, and damage-associated molecular patterns (DAMPs) are released, which induce immune responses by professional APCs, such as DCs (9–11). Upon activation, DCs internalize released Ag, process it, and trigger CD8⁺ T cell-dependent cellular immune responses (6, 12–14). Sterile necrotic cells possess the potential to activate innate inflammatory

responses and to mature DCs (14–16). Several studies showed that UV-irradiated secondary necrotic cells trigger Ag-specific CD8⁺ T cell responses in a TIR-IL1 β -independent (17) or CLEC9A-dependent (18) manner. Heat shock proteins (HSPs) (12, 19, 20), HMGB1 (13, 21), HMGN1 (22), uric acid (11), genomic DNA (23), and F-actin (24) have all been identified as endogenous DAMPs associated with necrosis, with the potential to induce immune responses.

However, recent studies have shown that, despite release of DAMPs, freeze-thawed (FT) necrotic tumor cells did not induce Ag-specific CD8⁺ T cell activation when injected into mice under sterile conditions in the absence of PAMPs (17, 25–27). These results indicate that the question of immunogenicity of necrotic cell death remains open. Further studies are needed to identify the mechanisms that control cross-priming of CD8⁺ T cells and generation of adaptive immune responses during necrotic cell death.

In the present study, we investigated the role of Ag donor, primary sterile necrotic cells in cross-priming of CD8⁺ T cells and in Ag-specific adaptive immune response generation. We showed that DCs pulsed with FT sterile necrotic cells failed to trigger Ag-specific CD8⁺ T cell-mediated immune responses in vivo. In contrast, when FT sterile necrotic cells were heated prior to pulsing onto DCs, they induced potent CD8⁺ T cell activation and protected mice from subsequent tumor challenges. We also showed that nonimmunogenic necrotic cells precluded CD8⁺ T cell activation, indicating the presence of mechanisms in Ag donor cells that can control cross-priming of CD8⁺ T cells and adaptive immune response generation. Using chromatography and mass-spectrometric approaches, we identified cellular peptidases, particularly dipeptidyl peptidase 3 (DPP-3; gi|244791124) and thimet oligopeptidase 1 (TOP-1; gi|239916005), that represent important components of this control mechanism in necrotic cells. We showed that purified DPP-3

Authorship note: Tamar Kapanadze and Miaojun Han, as well as Firouzeh Korangy and Tim F. Greten, contributed equally to this work.

Conflict of interest: The authors have declared that no conflict of interest exists.

Citation for this article: *J Clin Invest.* 2013;123(11):4755–4768. doi:10.1172/JCI65698.

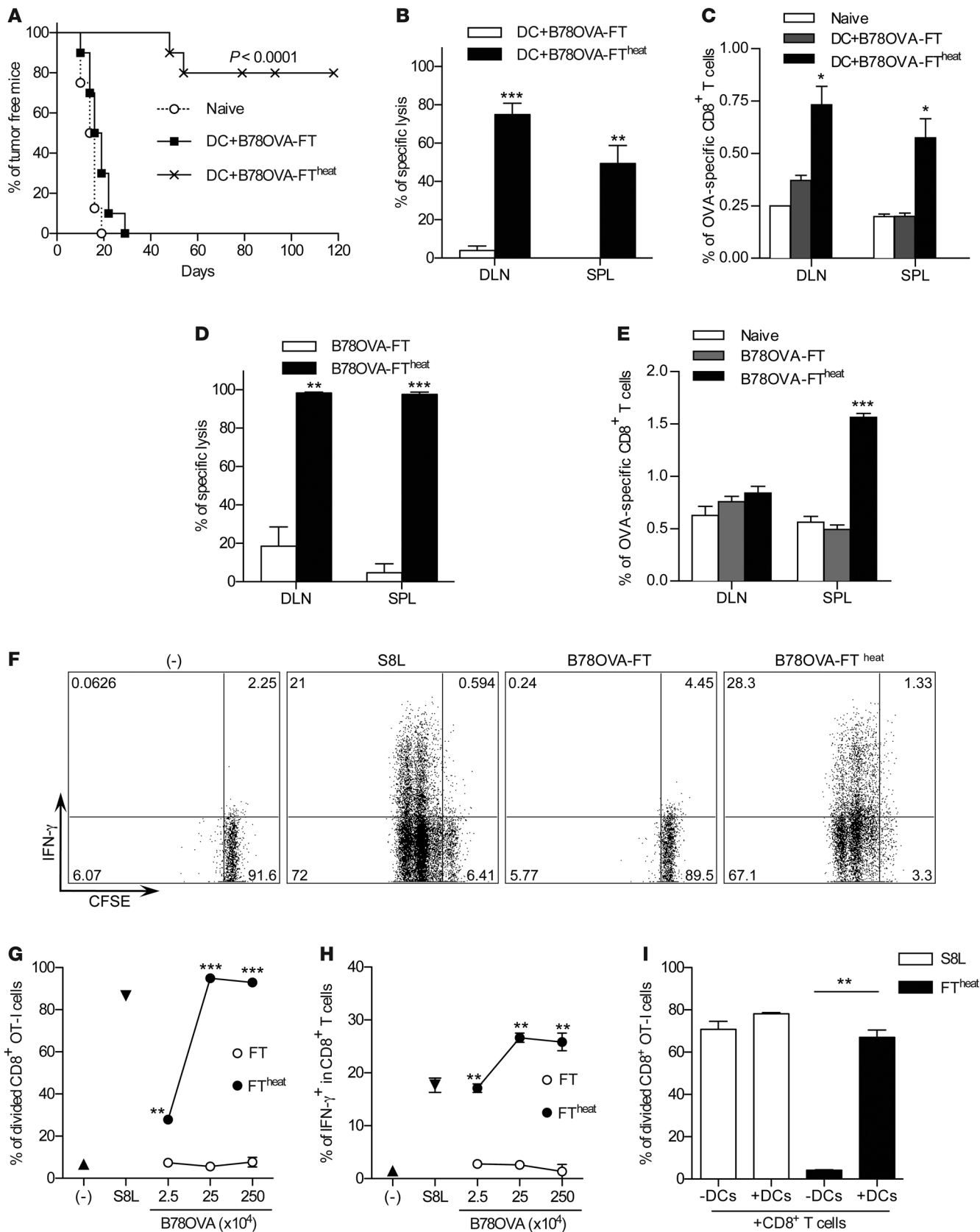




Figure 1

Primary FT necrotic cells do not induce CD8⁺ T cell activation. (A) On days 0 and 2, splenic CD11c⁺ DCs were pulsed with SF of B78OVA-FT or B78OVA-FT^{heat} cells. DCs were washed and injected into mice. On day 7, recipients were challenged with live B16OVA, and tumor growth was monitored. Data are from 2 independent experiments ($n = 8-10$ per group). $P < 0.0001$, log-rank (Mantel-Cox) test. (B and C) Mice were vaccinated as in A, and OVA-specific lysis (B) and percent OVA-specific CD8⁺ T cells (C) in draining LNs (DLN) and spleens (SPL) were determined on day 7. Data are from 1 representative of 2 experiments ($n = 3$ per group). (D and E) Mice were vaccinated with 5×10^6 B78OVA-FT or B78OVA-FT^{heat} cells on days 0 and 2. On day 7, OVA-specific lysis (D) and percent tetramer-positive cells (E) was determined. Data are representative of 3 experiments ($n = 3$ per group). (F-H) SF from B78OVA-FT was incubated at 70°C (FT^{heat}) and cultured in vitro with OT-I splenocytes. Proliferation and IFN- γ expression of CD8⁺ T cells was analyzed after 48 hours. (F) IFN- γ release by proliferating CD8⁺ OT-I cells. (G and H) Corresponding cumulative results. Data are representative of 3 independent experiments. (I) S8L or B78OVA-FT^{heat} cells (2.5×10^5) were cultured with OVA-specific CFSE-labeled CD8⁺ T cells with or without CD11c⁺ DCs, and T cell proliferation was analyzed. Results are representative of 3 independent experiments. * $P < 0.05$, ** $P < 0.01$, *** $P < 0.001$, Student's t test.

and TOP-1 prevented CD8⁺ T cell cross-priming with heated sterile necrotic cells in vitro and in vivo. DPP-3 and TOP-1 aborted peptide-based CD8⁺ T cell activation, which suggests that oligopeptides are their targets. We also showed that DPP-3 and TOP-1 lost their function when heated. The immunogenicity of heated sterile necrotic cells, besides peptidase inactivation, relies on proteasome function responsible for oligopeptide generation from cellular proteins and/or defective ribosomal products (DRiPs). This novel mechanism represents one more important example of how tightly adaptive immune response generation – especially cross-priming of CD8⁺ T cells – is controlled to avoid unwanted activation during cell death. Exploitation of this mechanism (i.e., inactivation of peptidases and generation of oligopeptides operating at the Ag processing and presentation levels) may be crucial for the design of efficient anticancer vaccination and therapeutic strategies.

Results

Primary FT necrotic cells do not induce CD8⁺ T cell activation. We assessed different types of necrotic cells for their potential to induce Ag-specific CD8⁺ T cell responses. DCs were loaded either with B78OVA cells that had undergone 3 FT cycles (B78OVA-FT) or with B78OVA-FT cells that were additionally heated (B78OVA-FT^{heat}), then injected into mice. All mice were challenged with live B16OVA tumor cells, and tumor-free survival was analyzed. While all mice developed tumors after vaccination with B78OVA-FT-loaded DCs, 80% of all DC-vaccinated mice survived more than 150 days when FT tumor cells were heated prior to pulsing (Figure 1A). Analysis of Ag-specific T cell responses corroborated our findings. In vivo CTL assay demonstrated higher Ag-specific lysis in mice injected with DCs loaded with B78OVA-FT^{heat} than with B78OVA-FT (Figure 1B). In addition, these mice showed higher numbers of Ag-specific T cells (Figure 1C). Similar results were obtained when B78OVA-FT and B78OVA-FT^{heat} cells were injected directly (without DCs): again, only when necrotic cells were heated after FT was potent Ag-specific lysis observed in vivo (Figure 1, D and E, and Supplemental Figure 1, A-D; supplemental material available online with this article; doi:10.1172/JCI65698DS1).

In order to examine the biological mechanism responsible for this observation, we tested necrotic tumor cells in vitro. Soluble fractions (SF) of B78OVA-FT or B78OVA-FT^{heat} cells were cultured with splenocytes from OT-I mice, and T cell activation was analyzed. Neither IFN- γ release nor proliferation of CD8⁺ T cells was seen with B78OVA-FT, whereas Ag-dependent responses were observed when SF of B78OVA-FT^{heat} cells (Figure 1, F-H) or whole B78OVA-FT^{heat} cells (Supplemental Figure 1, E and F) were used. Similar results were found with CT26OVA cells in vitro (Supplemental Figure 1, G and H). When immunogenic necrotic cells were cultured with purified CD8⁺ T cells alone (i.e., in the absence of DCs), proliferation was not observed (Figure 1I), which suggests that Ag cross-presentation by professional APCs is crucial for T cell activation.

Primary FT necrotic cells abort cross-priming of CD8⁺ T cells. We then sought to determine whether primary FT necrosis is immunologically a null event or whether it can actively block cross-priming of CD8⁺ T cells. To test this hypothesis, B78-FT and B78OVA-FT^{heat} were coinjected into mice on days 0 and 2, and Ag-specific T cell responses were determined by in vivo CTL assay on day 7. Addition of B78-FT tumor cells abrogated Ag-specific lysis in vivo (Figure 2A). Similarly, Ag-specific CD8⁺ T cell proliferation was reduced in vitro when B78-FT and B78OVA-FT^{heat} cells were cocultured with OT-I cells (Figure 2B). These results suggested that necrotic cells contain factors that preclude cross-priming of CD8⁺ T cells.

SF from B78-FT was trypsin digested and cultured with OT-I splenocytes in the presence of 20 $\mu\text{g/ml}$ OVA. Digested SF triggered Ag-specific proliferation and IFN- γ expression by CD8⁺ T cells in vitro (Figure 2, C and D), which suggests that trypsin-sensitive proteins are responsible for limiting CD8⁺ T cell activation. Trypsin alone had no influence on CD8⁺ T cell activation in the presence of OVA (data not shown). Next, we asked whether these proteins were also present in tumor cells other than mouse melanoma, and tested trypsin-digested SF from CT26-FT colon carcinoma (Figure 2, E and F) as well as human tumor cells and mouse embryonic fibroblasts (MEFs; Supplemental Figure 2, A-D). In all cases, trypsin digestion unmasked the ability to activate CD8⁺ T cells, suggestive of a general phenomenon that was not restricted to certain cell types.

Cells contain high-molecular weight factors capable of activating CD8⁺ T cells. SF of B78-FT tumor cells were fractionated using gel filtration, and individual fractions were tested for their ability to induce Ag-specific T cell responses in the presence of OVA. Unexpectedly, we observed robust CD8⁺ T cell activation after incubation of fractions 9-23 with OT-1 cells (Figure 3A). This result showed that SF from necrotic tumor cells also contained factors that potentially enhance Ag-specific immune responses in vitro (Figure 3A and Supplemental Figure 3A). Fractions 9-23, obtained using gel filtration, were pooled (referred to hereafter as F₉₋₂₃) and further characterized. First, we tested whether F₉₋₂₃ affects DC function or interacts with the Ag (Figure 3B). We found that preincubation of F₉₋₂₃ with DCs, or its addition later, did not enhance CD8⁺ T cell proliferation (Figure 3C). In contrast, even a short incubation of F₉₋₂₃ with Ag induced CD8⁺ T cell proliferation (Figure 3C). These results suggest that Ag and F₉₋₂₃ interaction is essential for triggering of T cell activation and less likely to be caused by a direct effect on APCs or T cells. At the same time, F₉₋₂₃ enhanced neither Ag uptake nor rapid protein elimination (Supplemental Figure 3, B and C).

Based on the observations that F₉₋₂₃ had a high molecular weight and did not affect APC or protein uptake, but rather influenced the Ag, we speculated that T cell activation ability might rely on

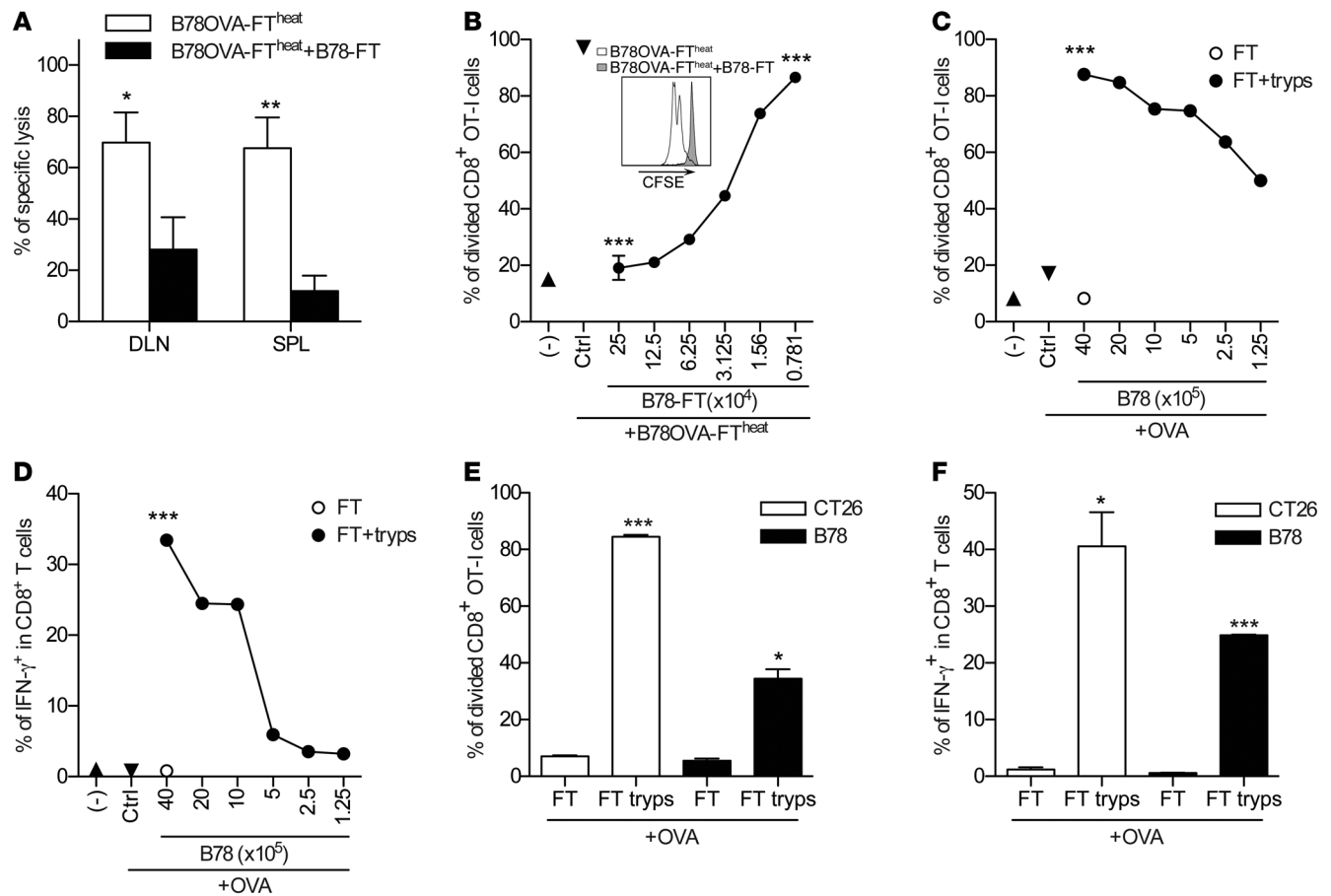


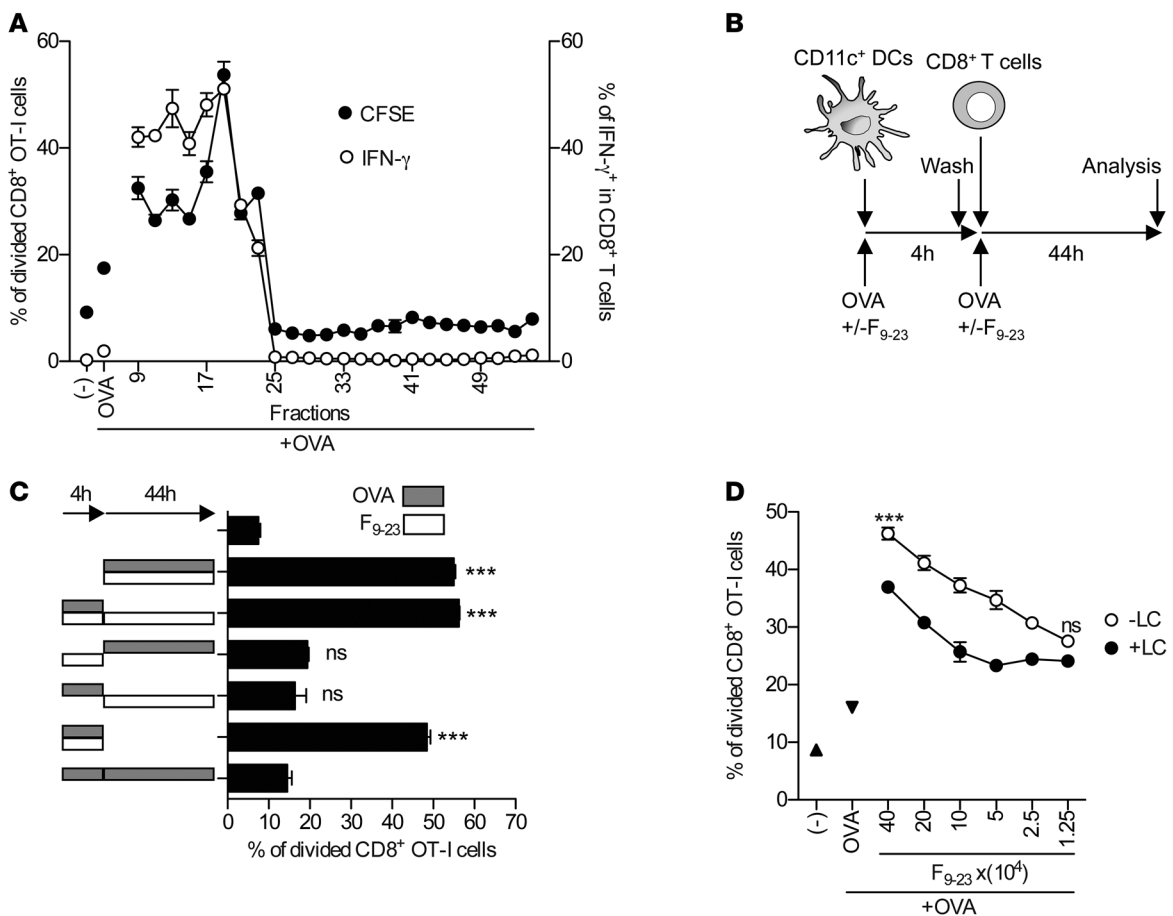
Figure 2 Primary FT necrotic cells abort cross-priming of CD8⁺ T cells. (A) B78OVA-FT^{heat} cells were mixed with B78-FT cells at a 1:8 ratio and injected into mice on days 0 and 2, so that each mouse was vaccinated with a total of 2 × 10⁶ B78OVA cells. Ag-specific immune responses were analyzed on day 7. Data are mean ± SEM of 2 pooled experiments (n = 3 per group). (B) SF of 2.5 × 10⁵ B78OVA-FT^{heat} cells was cultured in vitro with CFSE-labeled OT-I splenocytes, and titrated amount of SF from B78-FT was added. Proliferation of CD8⁺ T cells was analyzed after 48 hours. Data are representative of at least 3 independent experiments. Inset shows proliferation of OVA-specific CFSE-labeled CD8⁺ T cells cultured with B78OVA-FT^{heat} or B78OVA-FT^{heat} + B78-FT cells. (C and D) SF from B78-FT cells was trypsin digested and added at different dilutions to CFSE-labeled OT-I cells in the presence of 20 μg/ml OVA. Proliferation (C) and IFN-γ expression (D) of CD8⁺ T cells were analyzed 48 hours later. Data are representative of at least 3 experiments. (E and F) Trypsin-digested SF from CT26-FT or B78-FT cells were added to CFSE-labeled OT-I splenocytes in the presence of 20 μg/ml OVA, and Ag-specific proliferation (E) and IFN-γ expression (F) was tested. Data are representative of at least 3 experiments. *P < 0.05, **P < 0.01, ***P < 0.001, Student's *t* test (A and C–F) or 1-way ANOVA with Dunnett's multiple-comparison test (B).

the generation and/or chaperoning of oligopeptides. Because proteasome generates oligopeptides in cells, we tested this hypothesis by inhibiting proteasome activity in F₉₋₂₃ using lactacystin, an irreversible and highly specific proteasome inhibitor (28). When lactacystin-pretreated F₉₋₂₃ was added to the OT-I cell cultures in the presence of OVA, T cell proliferation was reduced (Figure 3D). Together, these results suggest that proteasome-dependent oligopeptide generation machinery might be responsible for Ag-specific T cell activation in the absence of a negative regulatory mechanism during primary sterile necrotic cell death.

F₃₇₋₄₅ characterization. In order to characterize and identify those proteins that prohibit cross-priming of CD8⁺ T cells, we used a F₉₋₂₃/OVA-dependent T cell activation assay as a platform for future experiments (Figure 4A). First, we tested the remaining fractions from our initial gel filtration (Figure 4A) and observed that T cell activation was strongly impaired in the presence of fractions 37–45 (Figure 4B and Supplemental Figure 4A). These fractions

were pooled and used for further characterization. Pre-exposure of F₃₇₋₄₅ to pH <4.0 at room temperature aborted its activity, as did incubation at 56 °C (partial) and 70 °C (complete) (Supplemental Figure 4, B–D). Next, we asked whether F₃₇₋₄₅ influences APCs or F₉₋₂₃/Ag (Figure 4C). F₃₇₋₄₅ blocked T cell activation only when it was present together with F₉₋₂₃ and Ag (Figure 4D). Preincubation of F₃₇₋₄₅ with DCs, or its addition later, did not abolish CD8⁺ T cell proliferation, which suggests that F₃₇₋₄₅ influences Ag (and/or F₉₋₂₃) rather than APCs and/or T cells.

Similarly, F₃₇₋₄₅ did not affect the uptake of Alexa Fluor 488-labeled OVA (OVA-A₄₈₈) by DCs in vitro (Supplemental Figure 3D). It did not eliminate OVA protein, in contrast to proteinase K, when cultured in vitro and assessed by Western blotting (Supplemental Figure 3E). These results suggested that complete elimination of antigenic material (i.e., protein) is not the mechanism by which F₃₇₋₄₅ influences cross-priming. This was further confirmed by our T cell activation assay results: prein-

**Figure 3**

Necrotic cells contain high-molecular weight factors capable of activating CD8⁺ T cells. (A) SF from B78-FT cells was fractionated by gel-filtration chromatography. Fractions were washed, adjusted to equal volumes, and added to the cultures of CFSE-labeled OT-I splenocytes in the presence of 20 μ g/ml OVA. Proliferation and IFN- γ expression of CD8⁺ T cells were analyzed after 48 hours. Data show 1 representative of 2 independent experiments. (B and C) Purified CD11c⁺ DCs (5×10^4) were precultured with F₉₋₂₃ or 20 μ g/ml OVA for 4 hours. DCs were then washed, and purified CFSE-labeled OT-I CD8⁺ T cells (1×10^5) were added and incubated for 44 hours in the presence or absence of F₉₋₂₃ and/or OVA, as indicated. Proliferation of Ag-specific CD8⁺ T cells was determined. Data are representative of 3 independent experiments. (D) F₉₋₂₃ was preincubated with lactacystin (LC) or DMSO, extensively washed, and added to OT-I splenocytes in the presence of 20 μ g/ml OVA. Proliferation of CD8⁺ T cells was analyzed after 48 hours. *** $P < 0.001$, 1-way ANOVA with Dunnett's multiple-comparison test (C) or with Bonferroni's paired-comparison test (D).

cubation of OVA with F₃₇₋₄₅ and subsequent heat inactivation did not reduce the ability of OVA to prime CD8⁺ T cells in the presence of F₉₋₂₃ (Figure 4, E and F).

DPP-3 and TOP-1 from necrotic cells preclude CD8⁺ T cell priming in vitro and in vivo. In order to identify the negative regulators of cross-priming in F₃₇₋₄₅, 5 additional chromatographic steps were performed (Supplemental Table 2). Fractions from the last chromatographic step were collected and tested in vitro for functional activity. Fractions Fx33-Fx36, which aborted CD8⁺ T cell priming (Figure 5, A and B), were digested with trypsin and labeled using iTraQ technology, and relative intensities of the label were evaluated after liquid chromatography-mass spectrometry/mass spectrometry (LC-MS/MS) analysis (Figure 5, C and D, Supplemental Table 1, and data not shown). Aliquots of the fractions were analyzed by SDS-PAGE. Fx33-Fx36 contained 2 dominant bands of approximately 75-85 kDa in size (Supplemental Figure 5A). Functional activity was most prominent in Fx34 (Figure 5,

A and B), which suggests that the proteins responsible for it are mostly localized in this fraction. In LC-MS/MS analysis of fractions Fx33-Fx36, we identified highly abundant proteins with high sequence coverage, most of which were peptidases (data not shown). Relative intensity analysis of the iTraQ label in these fractions — and comparison with the relative functional activity obtained from the T cell activation assay — revealed that the distribution of biologically active regulatory factors correlated well with the relative iTraQ intensities of DPP-3 and TOP-1 (Figure 5, A-D, and Supplemental Table 1). These peptidases were mostly localized in Fx33-Fx35, with the highest intensity seen in Fx34 (Figure 5, C and D, and Supplemental Table 1). In accordance with this, Fx34 showed the most prominent functional activity, whereas Fx33 and Fx35 were relatively less potent. Distribution of the relative reporter intensities of murine prolyl endopeptidase (gi|6755152) did not correlate to the distribution of searched functional activities in these fractions. Based on these results, we

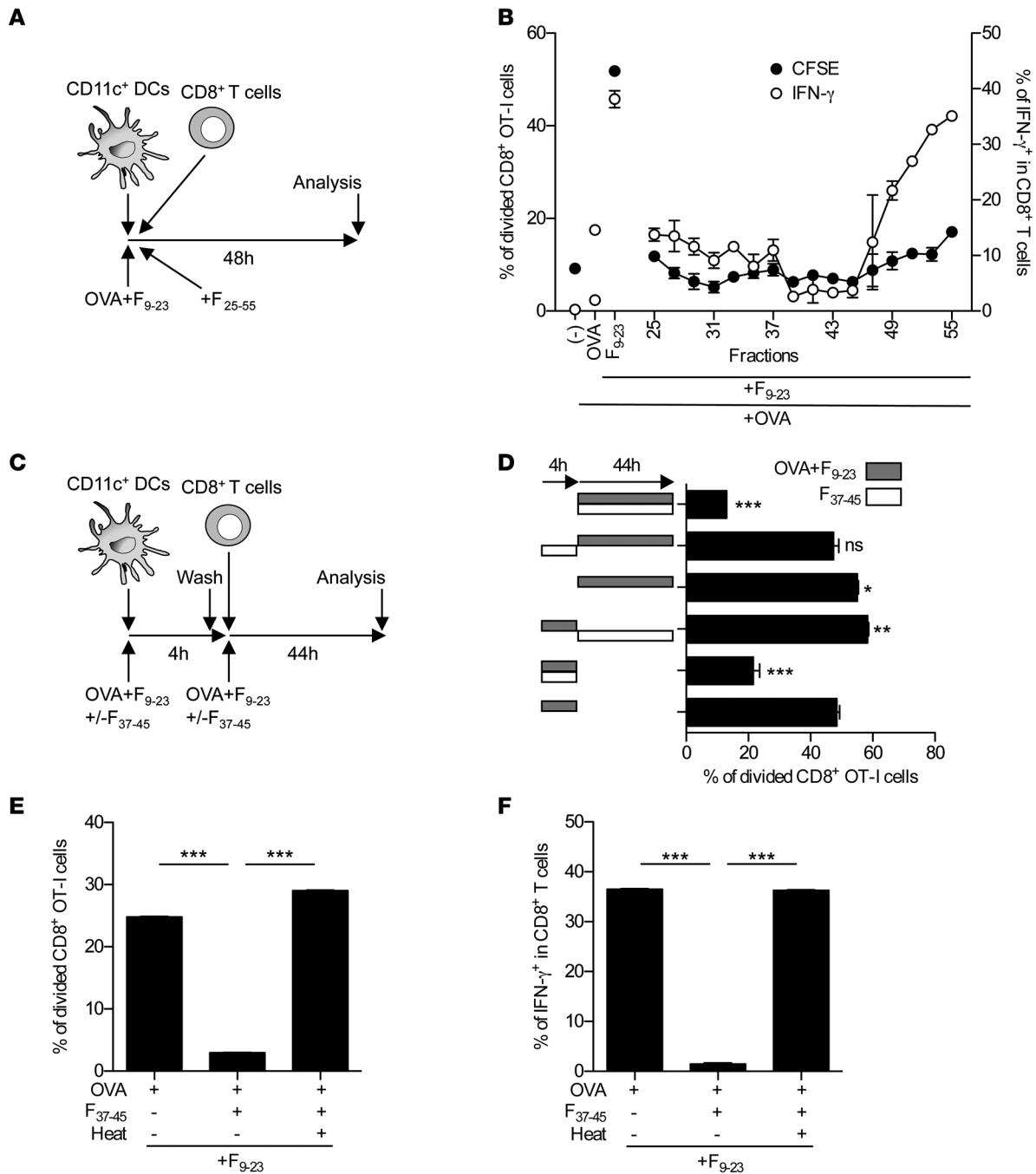


Figure 4

F₃₇₋₄₅ characterization. (A and B) Chromatographic fractions (see Figure 2E) were added to CFSE-labeled OT-I splenocytes in the presence of 20 μ g/ml OVA and F₉₋₂₃. Proliferation and IFN- γ expression of CD8⁺ T cells was analyzed after 48 hours. Data show 1 representative of 2 independent experiments. (C and D) Splenic CD11c⁺ DCs (5×10^4) were preincubated with F₉₋₂₃ and 20 μ g/ml OVA with or without F₃₇₋₄₅ for 4 hours. DCs were then washed, and purified CFSE-labeled OT-I CD8⁺ T cells (1×10^5) were added and incubated for 44 hours in the presence of F₃₇₋₄₅ and/or F₉₋₂₃ plus OVA, as indicated. Proliferation of Ag-specific CD8⁺ T cells was determined. (E and F) 20 μ g/ml OVA protein was incubated with F₃₇₋₄₅ overnight at 37°C and subsequently heated at 70°C for 1 hour as indicated. Samples were added to the CFSE-labeled OT-I cells in the presence of F₉₋₂₃, and CD8⁺ T cell activation was determined after 48 hours. Results are representative of 3 independent experiments. **P* < 0.05, ***P* < 0.01, ****P* < 0.001, 1-way ANOVA with Dunnett's multiple-comparison test (D) or Student's *t* test (E and F).

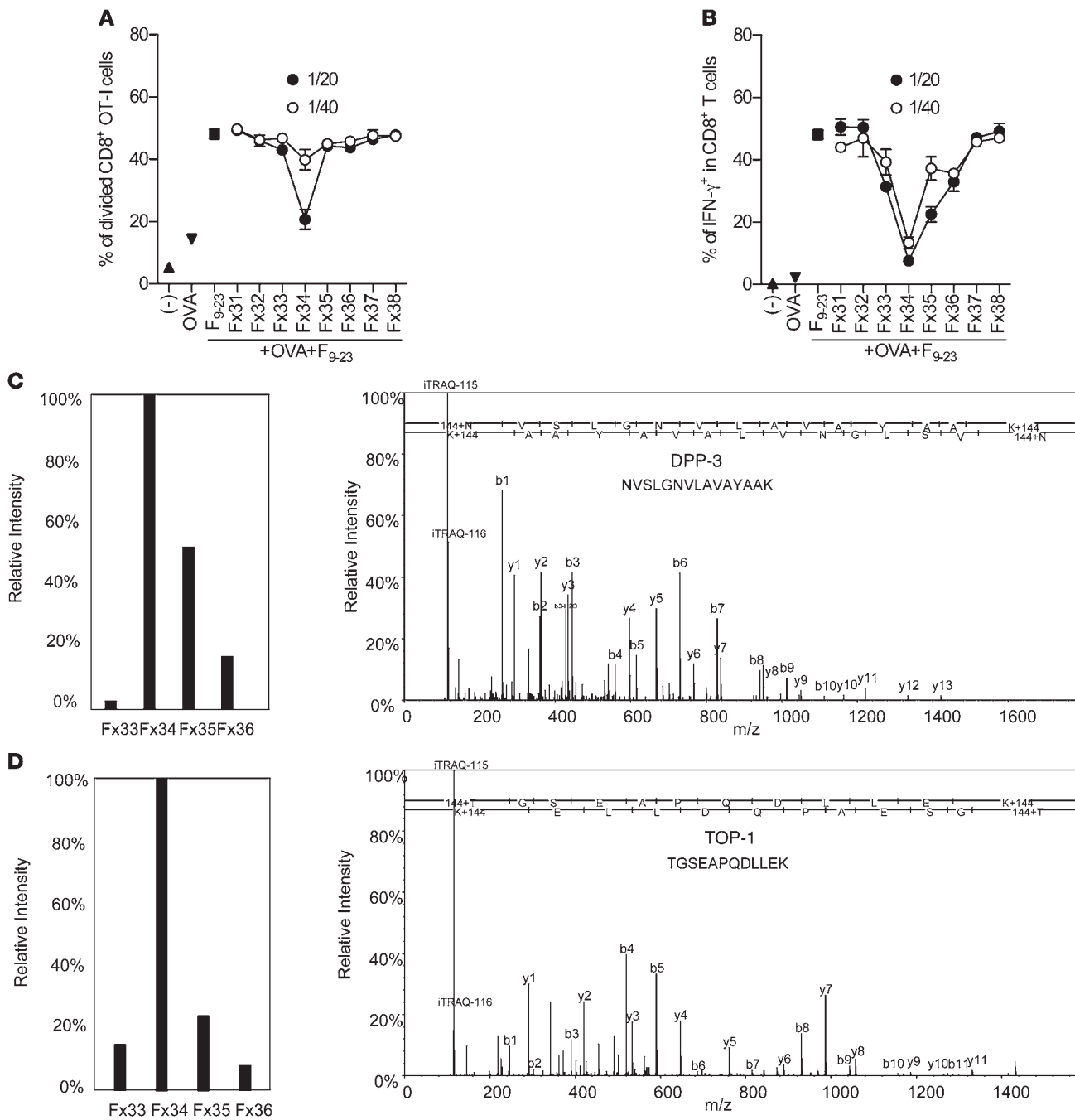


Figure 5 Purification and identification of peptidases controlling cross-priming of CD8⁺ T cells. (A and B) Fx fractions from anion exchange chromatography were collected, desalted, and concentrated. Titrated amounts of these fractions were added to the CFSE-labeled OT-I splenocytes in the presence of F₉₋₂₃ and 20 μg/ml OVA, and T cell activation was analyzed. Results are representative of 3 independent experiments. (C and D) Representative spectra of DPP-3 and TOP-1. Ions belonging to the y- and b-ion series are indicated. The iTRAQ-label region is shown magnified. The reporter ion labels 114, 115, 116, and 117 are replaced by the fraction numbers (Fx33, Fx34, Fx35, and Fx36, respectively) from anion exchange chromatography onto Resource-Q (GE). Relative intensities are indicated.

concluded that DPP-3 and TOP-1 correspond to potential candidate proteins and selected them for future analysis.

DPP-3 and TOP-1 are metallopeptidases involved in the cleavage of oligopeptides (29–33). TOP-1 has recently been shown to be responsible for the degradation of antigenic epitopes by remov-

ing N-terminal amino acids from peptides ranging from 8 to 17 amino acids (34, 35). DPP-3 was specifically shown to cleave Arg-Arg, Ala-Arg, Asp-Arg, and Tyr-Gly dipeptid residues from N termini of oligopeptides or proteins (29–31). Here, we cloned DPP-3 and TOP-1, after which they were expressed in *E. coli*, purified,

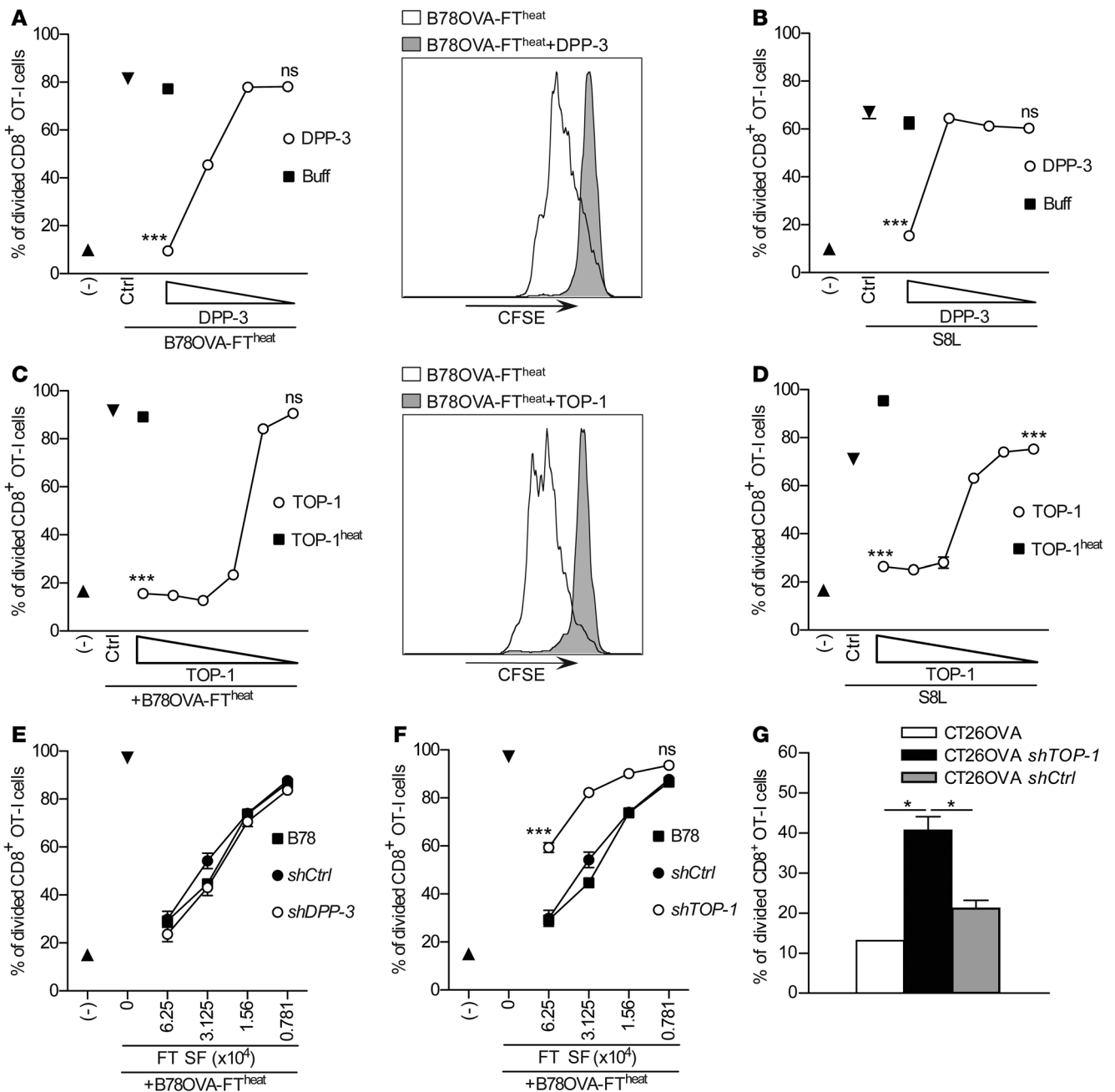
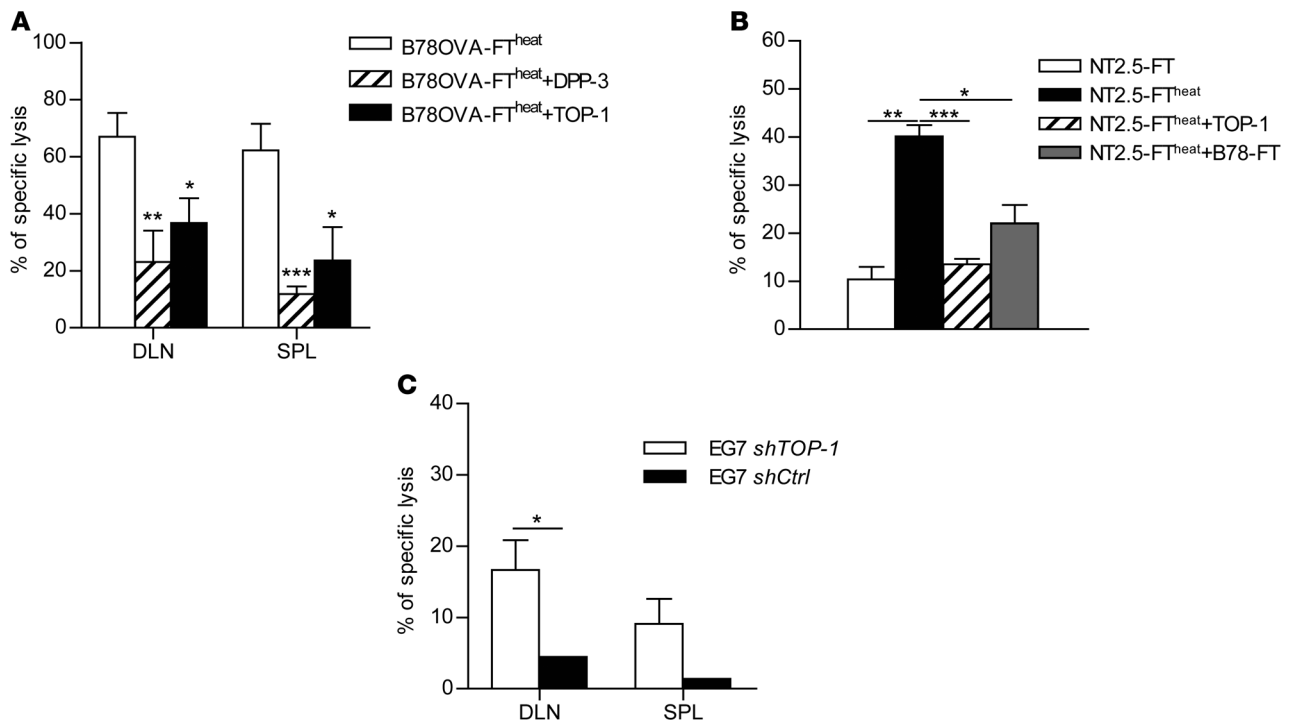


Figure 6

DPP-3 and TOP-1 preclude CD8⁺ T cell priming. Titrated amounts of recombinant DPP-3 (**A** and **B**) or TOP-1 (**C** and **D**) were added to the cultures of DCs and CD8⁺ T cells together with the SF from B78OVA-FT^{heat} (**A** and **C**) or S8L (**B** and **D**), and T cell proliferation was analyzed. Data are representative of 3 independent experiments. Histograms represent T cell proliferation corresponding to **A** and **C**. (**E** and **F**) SF of B78OVA-FT^{heat} was cultured with DCs and T cells. Titrated amounts of SF from B78-FT cells transfected with control, *TOP-1*, or *DPP-3* shRNA plasmids were added, and T cell activation was analyzed. Data are from 3 independent experiments. (**G**) γ -irradiated CT26OVA transfectants were cultured for 24 hours alone and then for 72 hours with CFSE-labeled OT-I cells. T cell proliferation was analyzed. Data are representative of 2 independent experiments. **P* < 0.05, ****P* < 0.001, 1-way ANOVA with Dunnett's multiple-comparison test (**A–D**) or with Bonferroni's paired-comparison test (**E** and **F**), or Student's *t* test (**G**).

and tested in vitro in CD8⁺ T cell activation assays. Recombinant DPP-3 and TOP-1 both aborted CD8⁺ T cell activation in vitro in a dose-dependent manner when supernatants of B78OVA-FT^{heat} cells were used (Figure 6, **A** and **C**). Heating of TOP-1 and/or DPP-3 abolished their activity (Figure 6C and data not shown),

which suggests that inactivation of these peptidases and protection of their substrates – oligopeptides – from degradation is one mechanism by which heated necrotic cells activate Ag-specific T cell responses. As expected, DPP-3 and TOP-1 aborted CD8⁺ T cell proliferation when mature OVA_{257–264} epitope (S8L) was used

**Figure 7**

DPP-3 and TOP-1 control CD8⁺ T cell priming in vivo. (A) B78OVA-FT^{heat} cells (2×10^6) were mixed with recombinant TOP-1 or DPP-3 and injected into mice on days 0 and 2, and Ag-specific immune responses were analyzed on day 7. Data are from 3 experiments ($n = 3$ per group). (B) NT2.5-FT^{heat} cells (5×10^6), mixed with recombinant TOP-1 or with B78-FT cells (1×10^7), were injected into mice on days 0, 2, and 4, and Ag-specific immune responses were analyzed on day 7. Data show 1 representative of 3 independent experiments ($n = 3$ per group). (C) Subcutaneously growing control or TOP-1 shRNA-transfected EG7 tumors were exposed to X-ray radiation (15 Gy), and Ag-specific immune responses were analyzed after 5 days. Data are from 2 experiments ($n = 3$ per group). * $P < 0.05$, ** $P < 0.01$, *** $P < 0.001$, Student's *t* test.

instead of B78OVA-FT^{heat} cells (Figure 6, B and D). shRNA-mediated knockdown of TOP-1 expression in B78 cells prior to necrosis induction partially reduced the regulatory effect, whereas silencing of DPP-3 had no effect (Figure 6, E and F), which suggests that these factors are redundant and can substitute for each other.

To test whether peptidases also control cross-presentation of Ags derived from tumor cells that have died by an alternate mechanism, we γ -irradiated CT26OVA cells in which TOP-1 expression was silenced. TOP-1 knockdown in γ -irradiated CT26OVA cells enhanced T cell proliferation (Figure 6G).

Mice vaccinated with B78OVA-FT^{heat} cells in the presence of recombinant DPP-3 or TOP-1 showed reduced Ag-specific killing (Figure 7A). Similar results were obtained when NT2.5 cells, which express the tumor Ag Her-2/neu (36), were used as a vaccine. Mice vaccinated with NT2.5-FT^{heat} cells, but not with NT2.5-FT cells, showed enhanced Ag-specific killing, which was reduced when TOP-1 was coinjected during vaccination (Figure 7B). Mice bearing control EG7 tumors (see Methods) or EG7 tumors in which TOP-1 expression was silenced showed enhanced Ag-specific immune responses when tumors were locally exposed to X-ray irradiation (Figure 7C). In summary, these results indicated that DPP-3 or TOP-1 can interfere with cross-priming of CD8⁺ T cells during sterile necrotic cell death in vitro and in vivo.

Proteasome-dependent cross-priming confirms the significance of the regulatory mechanism. We next investigated the mechanism of CD8⁺ T cell activation with B78OVA-FT^{heat} cells. Pretreatment of F₉₋₂₃ with lactacystin reduced T cell proliferation (Figure 3D), which suggests

that proteasome might be responsible for this effect. Therefore, we asked whether inhibition of proteasome in B78OVA cells prior to necrosis induction produces the same effects. Lactacystin treatment of B78OVA cells prior to development of necrosis reduced T cell activation ability of B78OVA-FT^{heat} in vitro (Figure 8A). Similarly, mice vaccinated with lactacystin-treated B78OVA-FT^{heat} cells showed reduced Ag-specific immune responses, in contrast to recipients of control B78OVA-FT^{heat} vaccination (Figure 8B). These results strongly support our hypothesis that DPP-3 and TOP-1 in Ag donor necrotic cells control cross-priming of CD8⁺ T cells, which itself relies partially on lactacystin-sensitive, proteasome-dependent oligopeptide generation.

Discussion

We hypothesized that cross-priming of CD8⁺ T cells and induction of adaptive immune responses during necrotic cell death does not solely rely on the simple release of DAMPs from dead cells, but is rather a complex and tightly controlled process. To unravel the mechanisms responsible for cross-priming and T cell activation, the antigenic source available for peptide-MHC-I complex generation and the cellular machineries influencing this source must be taken into account. Previously, 3 different forms of antigenic material were described for processing and presentation: (a) mature proteins (37, 38), (b) DRiPs (39), and (c) oligopeptides/proteasomal degradation products (40, 41). It was shown that DRiPs play a role in MHC-I-based direct presentation and ensure quick and efficient recognition of virally infected cells by effector T cells

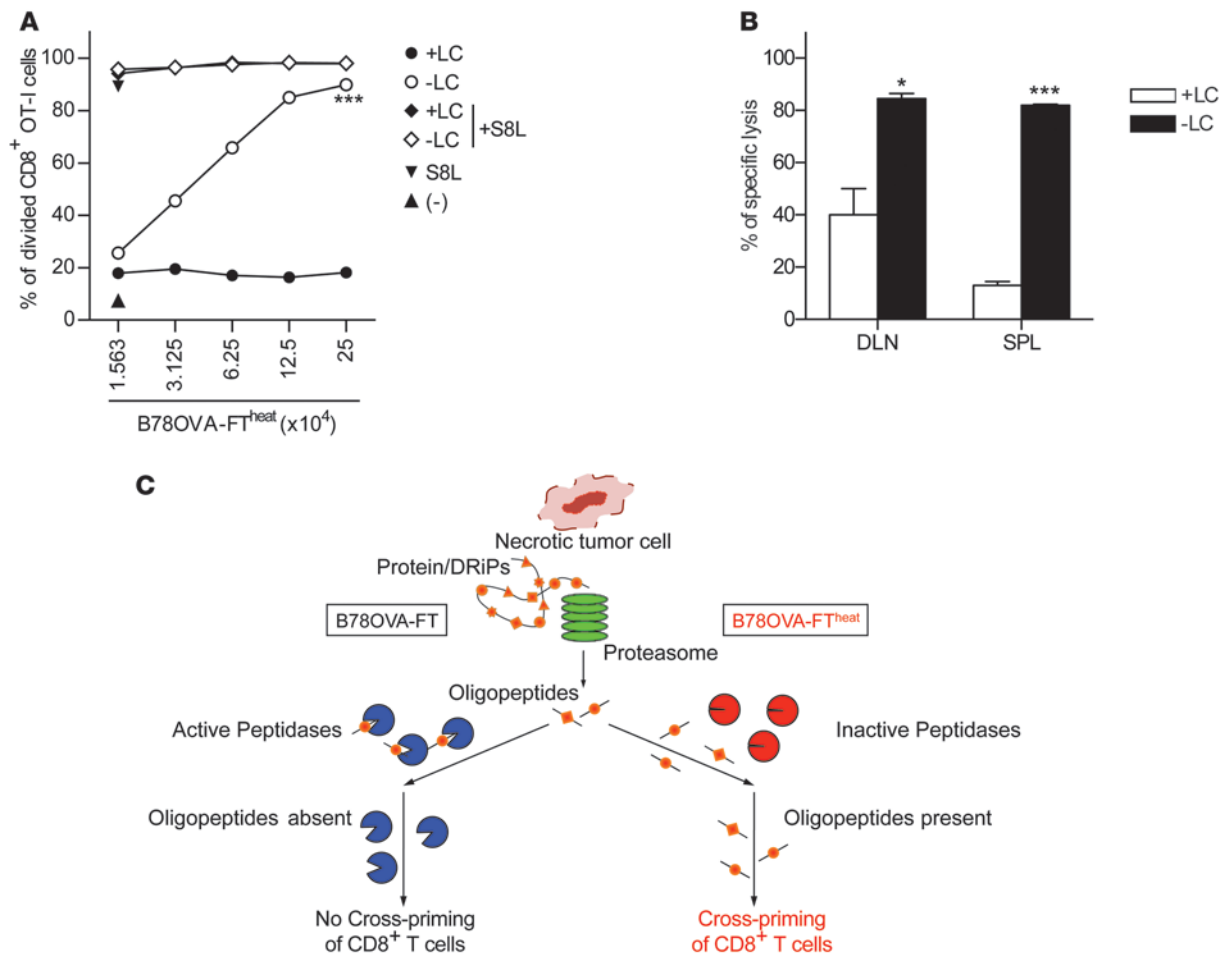


Figure 8

Proteasome-dependent cross-priming confirms the significance of the regulatory mechanism. **(A)** B780VA cells were preincubated with 50 μM lactacystin or DMSO at 37°C for 2 hours. Cells were washed and subjected to 3 FT cycles. SF from FT cells was collected and heat inactivated. Titrated amounts of LC-treated or control SF was cultured in vitro with purified DCs and T cells, and T cell activation was analyzed. Data are representative of 3 independent experiments. **(B)** B780VA cells were preincubated with 100 μM lactacystin or DMSO at 37°C for 2 hours. After washing, FT, and subsequent heating, 2 × 10⁶ cells were injected in mice on days 0 and 2, and Ag-specific immune responses were analyzed by in vivo CTL assay on day 7. Data are representative of 2 independent experiments. **(C)** Potential mechanism of immune response generation during sterile necrotic cell death and control of cross-priming by cellular peptidases. **P* < 0.05, ****P* < 0.001, 1-way ANOVA with Bonferroni's paired-comparison test **(A)** or Student's *t* test **(B)**.

(39), but their involvement in cross-presentation during primary, sterile, necrotic cell death has not previously been documented. Studies over the past 15 years have provided substantial support for the role of mature proteins (37, 38) in cross-presentation. However, non-physiologically high amounts of purified proteins are needed for cross-priming of Ag-specific CD8⁺ T cells in vitro (42, 43), which is unlikely to be reached under normal conditions. Moreover, despite the presence of the protein Ags in nonimmunogenic primary sterile necrotic cells, they fail to trigger CD8⁺ T cell-mediated adaptive immune responses in vivo (17, 25–27). Another form of the antigenic source described for cross-presentation is oligopeptides/proteasomal degradation products (40, 41). Oligopeptides are generated in the cells mostly via proteasomal degradation, and their size ranges from 2 to 25 amino acids (44, 45). Oligopeptides have a short half-life of a few seconds in the cytosol due to degradation by the cellular peptidases (45–47). Although it has been suggested that some oligopeptides might bind to chap-

erones, it is still not clear whether such binding can prevent them from further degradation (45). TOP-1 (35), TPPII (48), and PSA (49) were discovered to be responsible for oligopeptide degradation and elimination of the epitopes needed for the formation of peptide-MHC-I complexes and direct presentation in the cells.

Here, we described for the first time that a distinctive mechanism is operating at the subcellular level in Ag donor cells, which control cross-priming of CD8⁺ T cells during sterile primary necrosis. We provided evidence that during nonimmunogenic necrosis, cellular peptidases (including DPP-3 and TOP-1) retain their biological activity and eliminate oligopeptides necessary for cross-priming of naive CD8⁺ T cells. Addition of these recombinant proteins precluded T cell activation, even with the immunogenic (i.e., heated) necrotic cells, both in vitro and in vivo. Elimination of *TOP-1* caused reduction of this effect and enhanced T cell proliferation. However, when *DPP-3* was shut down, T cell proliferation was not affected, which suggests that these 2 differ-



ent peptidases might substitute for each other. This result might be additionally explained by the presence of other peptidases in Ag donor cells with similar function. Finally, necrotic cells might also contain other mechanisms, which can actively limit T cell cross-priming similar to these peptidases, but act in a manner independent of oligopeptide digestion.

When F₉₋₂₃ was treated with lactacystin, T cell proliferation was only impaired, not completely blocked (Figure 3D), which may be explained by incomplete blockade of the proteasome activity or by an alternate mechanism of oligopeptide generation — such as cathepsin S-mediated proteolysis (50) or the presence of cellular chaperones such as heat shock proteins (e.g., HSP90, HSP70, and gp96) — in these fractions.

When peptidases were inactivated in necrotic cells (achieved in our present study by heating, trypsin treatment, or gene-specific knockdown), they were no longer able to degrade oligopeptides, resulting in T cell activation. This activation was partially sensitive to lactacystin inhibition both *in vitro* and *in vivo*, which suggests that proteasome-dependent oligopeptide generation machinery is responsible for this effect and is only unmasked when negative regulatory mechanisms are eliminated. These results further support the idea that cross-priming of Ag-specific cells during primary necrosis is controlled at the level of proteasomal degradation products/oligopeptides and is specifically dependent on the functional status of their targeting machinery in Ag donor cells. It is worth mentioning that the presence of such mechanisms (namely, oligopeptide generation and peptidase activity) in necrotic cells further confirmed the already-recognized critical role of proteins and/or DRiPs in cross-presentation (37, 38, 51), since they are necessary for oligopeptide generation.

Another important aspect of our findings was that lack of T cell activation during nonimmunogenic sterile necrosis was not due to the absence of protein Ag, since even excess exogenous OVA protein (20 µg/ml) did not induce cross-priming with SF of nonimmunogenic necrotic cells. Some possible explanations for this effect include the absence of compartmentalized Ag with “eat-me” signals or other mechanisms that exclude protein from conventional uptake, processing, and cross-presentation pathways. Recently, tumor-infiltrating CD11c⁺CD11b⁺Ly6C^{hi} cells were shown to be critical for the induction of tumor-specific immune responses to tumors dying after anthracyclin treatment (52). While we were not able to study infiltrating immune cells at the vaccination site, we did not observe differences in the number of CD4⁺Foxp3⁺ Tregs, CD11b⁺Gr-1⁺ myeloid-derived suppressor cells, or CD11c⁺MHC II⁺ DCs in draining LNs and spleens from mice injected with untreated, necrotic, or heated necrotic tumor cells (data not shown).

F₃₇₋₄₅ failed to abort cross-priming when OVA-supplemented F₉₋₂₃ was preincubated with APCs, which suggests that either peptide-MHC-I complexes are separated from peptidase activity, or MHC-I protects and chaperones bound peptides from degradation. This latter phenomenon is further supported by previous studies (53).

Several studies have shown that secondary necrotic cells induced by UV irradiation trigger cross-priming of CD8⁺ T cells (17, 18), and this effect is mediated through CLEC9A signaling, which recognizes F-actin (24). However, in our studies, UV-irradiated B78OVA cells did not prime CD8⁺ T cells (data not shown). In contrast, enhanced T cell proliferation was observed with *TOP-1*-silenced, γ -irradiated cells, which suggests that peptidase activity in donor cells controls Ag cross-presentation upon different cell

death modalities. Notably, several clinical trials use DCs pulsed with FT tumor cells (54–56) or γ -irradiated tumor cells (57) as vaccines. Our findings suggest that T cell responses induced by these vaccines may be enhanced if tumor oligopeptidase activity is blocked in these settings.

A recent study has identified TOP-1 and nardilysin to be involved in the generation of mature epitopes for MHC-I direct presentation (58). Importantly, in our system, TOP-1 and DPP-3 both prevented cross-presentation of antigenic material from immunogenic necrotic cells *in vitro* and *in vivo*. This is also in accord with a previous study in which TOP-1 was shown to be involved in degradation of antigenic epitopes for MHC-I presentation (34, 35). One explanation for these potentially contradictory results might be the nature of the epitope. There might be some epitopes that will be destroyed by one peptidase, but trimmed by the others. This notion is also supported by our LC-MS/MS results, in which we identified at least 3 other peptidases with the potential to serve as regulators for Ag cross-presentation. In addition, the epitope/peptidase ratio or the length of the Ag-peptidase interaction might define whether it will be available for T cell activation.

Taken together, our present results identified a new important mechanism present in necrotic Ag donor cells that can define the immunological outcome of cell death (Figure 8C). We showed for the first time that during primary sterile nonimmunogenic necrosis, intracellular peptidases retain their biological activity and eliminate proteasomal degradation products, thereby preventing cross-priming of Ag-specific CD8⁺ T cells. We identified DPP-3 and TOP-1 as the 2 members of the peptidases family possessing such function. We also showed that heating of necrotic cells inactivates these peptidases and protects peptides from degradation, resulting in cross-priming of CD8⁺ T cells. Our study provides important evidence of basic biological mechanisms responsible for the control of CD8⁺ T cell activation at the level of Ag processing and cross-presentation.

Methods

Tumor cell lines. B78H1wt (B78) is an MHC-I negative clone of mouse melanoma (59). B78OVA and CT26OVA were generated as previously described to express a cell-associated, truncated version of OVA protein in the cytoplasm (60–62). B16OVA cells were provided by T. Schueler (DKFZ, Heidelberg, Germany). B16 cells expressing Flt3 ligand (B16FL) (63) were provided by D. Usharauli (Ghost Lab, NIAID/NIH, Bethesda, Maryland, USA). Immortalized *HMGB1*^{+/+} or *HMGB1*^{-/-} MEFs (64) were purchased from HMGBiotech. E.G7-OVA (EG7) cells were provided by N.P. Restifo (NCI/NIH, Bethesda, Maryland, USA). All cell lines were routinely tested for mycoplasma infection.

Mice. 8- to 10-week-old female C57BL/6 and FVB/n mice were obtained from Charles River Laboratories or from NCI Frederick. Previously described OVA TCR transgenic OT-I mice (65, 66) were from M.G. Sauer (Medizinische Hochschule Hannover, Hannover, Germany). Mice were maintained under specific pathogen-free conditions.

In vitro tumor cell preparation. Tumor cells were harvested, washed, resuspended in PBS at a concentration of 1.5×10^8 cells/ml, and exposed to 3 FT cycles (nonimmunogenic necrosis). Necrosis was confirmed by trypan blue staining, and cells were immediately used for further experiments. Alternatively, cell suspensions exposed to 3 FT cycles were centrifuged at 16,000 g for 20 minutes. After centrifugation of the pellet, cellular debris was discarded, and supernatant (i.e., SF) was collected. For chromatography, SF was centrifuged additionally at 28,000 g for 2 hours and stored at -20°C. Where indicated, whole necrotic cells or SF were heated at 70°C for



1 hour in order to induce immunogenic necrosis. In separate experiments, cells were treated with 50–100 μM lactacystin (Calbiochem) or DMSO for 2 hours at 37°C to inhibit proteasome activity. After extensive washing in fresh DMEM and PBS, immunogenic necrosis was induced as described above. CT26OVA transfectants (Figure 6G) were irradiated with 75 Gy to induce cell death and were used as a vaccine.

Trypsin digestion of necrotic tumor cells. Sequencing-grade modified trypsin (20 μg ; Promega) was activated in 100 μl buffer (Promega) at 30°C for 10 minutes and mixed with 200 μl SF in the presence of 20 mM NH_4HCO_3 . Samples were digested overnight at 37°C, washed, and concentrated through a Microcon filtration device (10-kDa molecular weight cutoff membrane; Millipore), washed in PBS, and concentrated. Concentrate was collected for further analysis or for experiments.

DC and T cell purification. BL6 mice were injected with 5×10^6 B16 cells expressing Flt3 ligand. After 12–14 days, single-cell suspensions from spleen were labeled with anti-CD11c antibody bound to the magnetic beads, and CD11c⁺ cells were isolated using AutoMACS technology (Miltenyi Biotech) according to the manufacturer's instructions. The purity of the cells after separation was 97%.

CD8⁺ OVA-specific T cells were purified from the spleens and LNs of OT-I mice. Single-cell suspensions were labeled with CFSE, then stained using mouse untouched CD8⁺ T cell isolation kit (Miltenyi Biotech). Untouched CD8⁺ T cells were purified using AutoMACS technology. The purity of CD8⁺ T cells exceeded 97%.

In vitro IFN- γ secretion and proliferation assay. Whole necrotic cells, SF, chromatographic fractions, and recombinant DPP-3 or TOP-1 were cultured in vitro with CFSE-labeled 2.5×10^5 OT-I splenocytes or 5×10^4 CD11c⁺ splenic DCs and 1×10^5 CD8⁺ OT-I cells for 48 hours, and IFN- γ secretion, proliferation, or both was determined using intracellular cytokine staining (Pharmingen) in combination with CFSE (Molecular Probes) labeling according to the manufacturer's instructions. 20 $\mu\text{g}/\text{ml}$ OVA protein (Worthington), 10 pM S8L (OVA₂₅₇₋₂₆₄; Biosynthon), or OVA-expressing necrotic tumor cells were used as Ags.

In the experiments described in Figure 3, B and C, and Figure 4, C and D, 5×10^4 CD11c⁺ splenic DCs were preincubated with Ag and/or fractions for 4 hours, washed in complete RPMI, and cultured with CFSE-labeled OVA-specific T cells for an additional 44 hours in the presence of fractions and/or Ag. T cell proliferation was analyzed 2 days later using flow cytometry.

Vaccination protocols and tumor treatments in vivo. Mice were vaccinated with the indicated number of necrotic cells subcutaneously in the left flank. Naive mice were used as a negative control. Ag-specific immune response was analyzed at 18 (OVA specific) or 48 (Her-2/neu specific) hours by in vivo CTL assay or by K^b-S8L tetramer staining (synthesized by the NIH Tetramer Facility at Emory University) on the indicated days after vaccination in draining LNs and spleens, as previously described (67, 68). In experiments where prophylactic vaccination was tested, vaccinated mice were challenged in the opposite flank using 1×10^4 live B16OVA cells, and tumor growth was monitored. A single radiation dose of 15 Gy was delivered to subcutaneously growing EG7 tumors in the right hind leg with a X-RAD 320 X-ray irradiator (Precision X-Ray) using 2.0-mm aluminum filtration (300 kV peak) at a dose of 2.8 Gy/minute. Ag-specific T cell responses were analyzed after 5 days.

Protein purification and identification using chromatography. For identification of Veto factors, a 6-step purification procedure was performed (Supplemental Table 2). Each step was followed by washing and concentration of the purification product through Amicon Ultra-15 or Ultra-4 centrifugal filters (30-kDa molecular weight cutoff; Millipore). Fractions from the last step were used for functional study, PAGE, iTraQ labeling, and LC-MS/MS analysis.

iTraQ labeling of peptides. Briefly, after extraction of equal aliquots from the Ressource-Q fractions using the method of Wessel and Flügge (69), iTraQ

labeling of peptides was performed according to the manufacturer's protocol (Applied Biosystems). The protein was digested at a protein/protease ratio of 50:1, and a maximum of 20 μg was labeled per label vial for 2 hours. A small aliquot, usually less than 0.1%, was used to confirm the minimum percentage of peptide labeling (>97%) using a 30-minute gradient and the Orbitrap LTQ XL mass spectrometer. Labeled fractions were then combined, desalted onto RP15, and used for LC-MS/MS.

LC-MS/MS analysis and database searching. LC-MS/MS was performed on an Acquity Ultra Performance LC-system (Waters Corp.) connected to an Orbitrap LTQ XL mass spectrometer (Thermo Scientific). Peptides were flushed onto a C₁₈ precolumn (5 μm Symmetry C₁₈, 180 $\mu\text{m} \times 20$ mm; Waters Corp.) at a flow rate of 15 $\mu\text{l}/\text{min}$ and washed at constant flow for 3 minutes. Peptides were then separated on an analytical column (1.7 μm BEH130, 75 $\mu\text{m} \times 150$ mm; Waters Corp.) with UPLC buffer A (0.1% formic acid in water) and UPLC buffer B (0.1% formic acid in acetonitrile) via linear A-B gradients over 2 hours from 0%–25% at a flow rate of 300 nl/min controlled with AcquityUPLC software (version 1.22). Data-dependent acquisition of MS and MS/MS data was controlled using Xcalibur software (version 2.1; Thermo Scientific). Doubly and triply charged peptide ions were automatically selected and fragmented with *m/z*-dependent collision energy settings. The raw data files were processed using Mascot Daemon software (version 2.3.2). Database searches were carried out with Mascot using the NCBI database 120302, using the following settings: enzyme, trypsin; maximum missed cleavages, 1; fixed modifications, carbamidomethyl (Cys), iTraQ K, iTraQ N, and variable oxidation (Met); peptide tolerance, 5 ppm; MS/MS tolerance, 0.1 Da. Scaffold (version Scaffold_3_00_03; Proteome Software Inc.) was used to validate MS/MS-based peptide and protein identifications. Proteins were only accepted as identified when at least 3 unique peptides showed 95% confidence and the total protein confidence was at least 95%. Peptide probabilities were specified by the Peptide Prophet algorithm (70), and protein probabilities were assigned by the Protein Prophet algorithm (71). Relative reporter intensities were calculated using the raw data files and QualBrowser software (Thermo Scientific).

PAGE and Western blotting. OVA protein (120 ng) was incubated at 37°C in the presence of different fractions or 1 μg proteinase K (Roche) for the indicated times. After incubation, samples (corresponding to 30 ng OVA) were resuspended in loading buffer, heated, and loaded on SDS-gel. After PAGE and blotting, membranes were stained with rabbit anti-OVA antibody (Chemicon) and with HRP-conjugated goat anti-rabbit antibody (Rockland). Membranes were developed using ECL detection reagent (Amersham) and analyzed in MultiImage II analyser (Alpha Inotech).

For PAGE, 10 μl of each chromatographic fraction was resuspended in sample loading buffer, heated, and loaded on 12% SDS-gel. After electrophoresis, gels were stained in Coomassie blue and visualized in Gel Doc 2000 (Bio-Rad Laboratories).

Uptake experiments. CD11c⁺ splenic DCs were cultured at 37°C in vitro with 5 $\mu\text{g}/\text{ml}$ OVA-A₄₈₈ (Molecular Probes) in the presence of different fractions, and OVA-A₄₈₈ uptake was analyzed using flow cytometry.

Generation of shRNA-transfected cells. For gene silencing, MISSION shRNA technology was used. TRC2-pLKO-puro nontarget shRNA plasmid DNA control or bacterial stocks expressing vector coding following shRNA sequences (Supplemental Table 3) were purchased from Sigma-Aldrich. Plasmid DNA was purified and used for transfection. B78, EG7, or CT26OVA cells (2×10^5) were cultured in antibiotic-free medium. After 24 hours, DNA (shRNA plasmids) and Lipofectamine (Invitrogen) were mixed in Optimem medium (Invitrogen) for 20 minutes at room temperature and added to cell culture. Stable transfectants were generated and maintained under G418 selection. Efficiency of the gene silencing was tested by quantitative real-time RT-PCR using the following primers: *TOP-1* forward, 5'-GCTCCCGGAGGACTTCTG-3'; *TOP-1* reverse, 5'-GCAGGGACAC-



TAGCTCCTTC-3'; *DPP-3* forward, 5'-CTGGCGAAGGACTCGTTACC-3'; *DPP-3* reverse, 5'-AGCAGTACCGTATCCCTTAGG-3'.

Cloning and purification of recombinant proteins. HA tag with linker was amplified from Jc1-HAHA-L-P7 (provided by T. Pietschmann, HZI, Hannover, Germany) using PCR. The 97-bp amplified fragment was purified from gel using QIAquick Gel extraction Kit (Qiagen), digested with *Bam*HI and *Eco*RI, and ligated into pHis3-TOP (provided by L.R. Travassos, Federal University of Sao Paulo, Sao Paulo, Brazil). *DPP-3* was excised from pSPORT6-DPP-3 (I.M.A.G.E. full-length cDNA Clone IRAVp968G117D, Source BioScience Life Sciences) using *Eco*RI and *Xho*I and cloned into pHis3 vector. The resulting pHis3-DPP-3 was digested using *Bam*HI and *Eco*RI, and HA tag and linker was ligated on the N terminus of the construct to generate pHis3-HAHA-DPP-3. *DPP-3* and TOP-1 were expressed in *E. coli* BL21(DE3)pLysS (Stratagene) and purified using Ni-NTA agarose beads (Qiagen). LPS was removed using Detoxi-Gel endotoxin-removing columns (Pierce) according to the manufacturer's instructions. Purified protein was aliquoted and stored at -20°C for further experiments.

Statistics. Experimental results are expressed as mean ± SEM. Significance of differences between 2 groups was calculated using Student's unpaired 2-tailed *t* test, with confidence interval of up to 95%. For comparisons among more than 2 groups, 1-way ANOVA followed by Dunnett's or Bonferroni's multiple-comparison tests was used. Tumor-free survival was analyzed using log-rank (Mantel-Cox) test. A *P* value less than 0.05 was considered significant.

Study approval. Animal studies were approved by the local Animal Care and Use Committee (license nos. 06/1195 and MOB-010).

Acknowledgments

We thank L.R. Travassos for pHis3-TOP construct; T. Pietschmann for Jc1-HAHA-L-P7; D. Usharauli for B16Flt3L cells; T. Schueler for B16OVA cells; N.P. Restifo for EG7 cells; NIH Tetramer Facility at Emory University for generation of K^b-S8L tetramer; J. Hartley and T. Taylor (PEL/NCI Frederick/NIH) for suggestions in recombinant protein expression and purification; D. Mannstein (MHH, Hannover, Germany) for advice in chromatography strategies; J. Luo (NCI/NIH) for advice in gene knockdown studies; and J.A. Berzofsky (NCI/NIH) for critical reading, comments, and suggestions on the manuscript. This research was supported (in part) by the Intramural Research Program of the NIH, NCI, Center for Cancer Research and by the Networking Fund of the Helmholtz Association within the Helmholtz Alliance on Immunotherapy of Cancer to M.P. Manns.

Received for publication July 9, 2012, and accepted in revised form August 8, 2013.

Address correspondence to: Tim F. Greten or Firouzeh Korangy, Gastrointestinal Malignancy Section, Medical Oncology Branch, NCI/NIH, Building 10, Room 12N226, 9000 Rockville Pike, Bethesda, Maryland 20892, USA. Phone: 301.451.4723; Fax: 301.402.0172; E-mail: tim.greten@nih.gov (T.F. Greten), firouzeh.korangy@nih.gov (F. Korangy).

- Lin ML, Zhan Y, Villadangos JA, Lew AM. The cell biology of cross-presentation and the role of dendritic cell subsets. *Immunol Cell Biol*. 2008;86(4):353–362.
- Carbone FR, Bevan MJ. Class I-restricted processing and presentation of exogenous cell-associated antigen in vivo. *J Exp Med*. 1990;171(2):377–387.
- Bevan MJ. Cross-priming for a secondary cytotoxic response to minor H antigens with H-2 congenic cells which do not cross-react in the cytotoxic assay. *J Exp Med*. 1976;143(5):1283–1288.
- Steinman RM. Dendritic cells in vivo: a key target for a new vaccine science. *Immunity*. 2008;29(3):319–324.
- Iwasaki A, Medzhitov R. Regulation of adaptive immunity by the innate immune system. *Science*. 2010;327(5963):291–295.
- Iyoda T, et al. The CD8⁺ dendritic cell subset selectively endocytoses dying cells in culture and in vivo. *J Exp Med*. 2002;195(10):1289–1302.
- Blander JM, Medzhitov R. Toll-dependent selection of microbial antigens for presentation by dendritic cells. *Nature*. 2006;440(7085):808–812.
- Robinson MJ, Sancho D, Slack EC, LeibundGut-Landmann S, Reis e Sousa C. Myeloid C-type lectins in innate immunity. *Nat Immunol*. 2006;7(12):1258–1265.
- Matzinger P. Tolerance, danger, and the extended family. *Annu Rev Immunol*. 1994;12:991–1045.
- Gallucci S, Lolkema M, Matzinger P. Natural adjuvants: endogenous activators of dendritic cells. *Nat Med*. 1999;5(11):1249–1255.
- Shi Y, Evans JE, Rock KL. Molecular identification of a danger signal that alerts the immune system to dying cells. *Nature*. 2003;425(6957):516–521.
- Binder RJ, Srivastava PK. Peptides chaperoned by heat-shock proteins are a necessary and sufficient source of antigen in the cross-priming of CD8⁺ T cells. *Nat Immunol*. 2005;6(6):593–599.
- Rovere-Querini P, et al. HMGB1 is an endogenous immune adjuvant released by necrotic cells. *EMBO Rep*. 2004;5(8):825–830.
- Sauter B, Albert ML, Francisco L, Larsson M, Somersan S, Bhardwaj N. Consequences of cell death: exposure to necrotic tumor cells, but not primary tissue cells or apoptotic cells, induces the maturation of immunostimulatory dendritic cells. *J Exp Med*. 2000;191(3):423–434.
- Kono H, Chen CJ, Ontiveros F, Rock KL. Uric acid promotes an acute inflammatory response to sterile cell death in mice. *J Clin Invest*. 2010;120(6):1939–1949.
- Chen CJ, Kono H, Golenbock D, Reed G, Akira S, Rock KL. Identification of a key pathway required for the sterile inflammatory response triggered by dying cells. *Nat Med*. 2007;13(7):851–856.
- Janssen E, et al. Efficient T cell activation via a Toll-Interleukin 1 Receptor-independent pathway. *Immunity*. 2006;24(6):787–799.
- Sancho D, et al. Identification of a dendritic cell receptor that couples sensing of necrosis to immunity. *Nature*. 2009;458(7240):899–903.
- Shi H, et al. Hyperthermia enhances CTL cross-priming. *J Immunol*. 2006;176(4):2134–2141.
- Somersan S, Larsson M, Fonteneau JF, Basu S, Srivastava P, Bhardwaj N. Primary tumor tissue lysates are enriched in heat shock proteins and induce the maturation of human dendritic cells. *J Immunol*. 2001;167(9):4844–4852.
- Yang H, et al. Programmed necrosis induced by asbestos in human mesothelial cells causes high-mobility group box 1 protein release and resultant inflammation. *Proc Natl Acad Sci U S A*. 2010;107(28):12611–12616.
- Yang D, et al. High-mobility group nucleosome-binding protein 1 acts as an alarmin and is critical for lipopolysaccharide-induced immune responses. *J Exp Med*. 2012;209(1):157–171.
- Ishii KJ, et al. Genomic DNA released by dying cells induces the maturation of APCs. *J Immunol*. 2001;167(5):2602–2607.
- Ahrens S, et al. F-actin is an evolutionarily conserved damage-associated molecular pattern recognized by DNGR-1, a receptor for dead cells. *Immunity*. 2012;36(4):635–645.
- Obeid M, et al. Calreticulin exposure dictates the immunogenicity of cancer cell death. *Nat Med*. 2007;13(1):54–61.
- Casares N, et al. Caspase-dependent immunogenicity of doxorubicin-induced tumor cell death. *J Exp Med*. 2005;202(12):1691–1701.
- Scheffer SR, et al. Apoptotic, but not necrotic, tumor cell vaccines induce a potent immune response in vivo. *Int J Cancer*. 2003;103(2):205–211.
- Craiu A, et al. Lactacystin and clasto-lactacystin beta-lactone modify multiple proteasome beta-subunits and inhibit intracellular protein degradation and major histocompatibility complex class I antigen presentation. *J Biol Chem*. 1997;272(20):13437–13445.
- Lee CM, Snyder SH. Dipeptidyl-aminopeptidase III of rat brain. Selective affinity for enkephalin and angiotensin. *J Biol Chem*. 1982;257(20):12043–12050.
- Fukasawa K, Fukasawa KM, Kanai M, Fujii S, Hirose J, Harada M. Dipeptidyl peptidase III is a zinc metallo-exopeptidase. Molecular cloning and expression. *Biochem J*. 1998;329(pt 2):275–282.
- Ellis S, Nuenke JM. Dipeptidyl arylamidase III of the pituitary. Purification and characterization. *J Biol Chem*. 1967;242(20):4623–4629.
- Camargo AC, et al. Structural features that make oligopeptides susceptible substrates for hydrolysis by recombinant thimet oligopeptidase. *Biochem J*. 1997;324(pt 2):517–522.
- Barrett AJ, et al. Thimet oligopeptidase and oligopeptidase M or neurolysin. *Methods Enzymol*. 1995;248:529–556.
- York IA, et al. The cytosolic endopeptidase, thimet oligopeptidase, destroys antigenic peptides and limits the extent of MHC class I antigen presentation. *Immunity*. 2003;18(3):429–440.
- Saric T, Graef CI, Goldberg AL. Pathway for degradation of peptides generated by proteasomes: a key role for thimet oligopeptidase and other metallo-peptidases. *J Biol Chem*. 2004;279(45):46723–46732.
- Ercolini AM, et al. Recruitment of latent pools of high-avidity CD8⁺ T cells to the antitumor immune response. *J Exp Med*. 2005;201(10):1591–1602.
- Basta S, Stoessel R, Basler M, van den Broek M, Groettrup M. Cross-presentation of the long-lived lymphocytic choriomeningitis virus nucleoprotein does not require neosynthesis and is enhanced via heat shock proteins. *J Immunol*. 2005;175(2):796–805.



38. Norbury CC, et al. CD8+ T cell cross-priming via transfer of proteasome substrates. *Science*. 2004; 304(5675):1318–1321.
39. Yewdell JW. DRiPs solidify: progress in understanding endogenous MHC class I antigen processing. *Trends Immunol*. 2011;32(11):548–558.
40. Lev A, et al. The exception that reinforces the rule: crosspriming by cytosolic peptides that escape degradation. *Immunity*. 2008;28(6):787–798.
41. Kunisawa J, Shastri N. Hsp90alpha chaperones large C-terminally extended proteolytic intermediates in the MHC class I antigen processing pathway. *Immunity*. 2006;24(5):523–534.
42. Reis e Sousa C, Germain RN. Major histocompatibility complex class I presentation of peptides derived from soluble exogenous antigen by a subset of cells engaged in phagocytosis. *J Exp Med*. 1995; 182(3):841–851.
43. Burgdorf S, Kautz A, Bohnert V, Knolle PA, Kurts C. Distinct pathways of antigen uptake and intracellular routing in CD4 and CD8 T cell activation. *Science*. 2007;316(5824):612–616.
44. Goldberg AL, Cascio P, Saric T, Rock KL. The importance of the proteasome and subsequent proteolytic steps in the generation of antigenic peptides. *Mol Immunol*. 2002;39(3–4):147–164.
45. Rock KL, York IA, Goldberg AL. Post-proteasomal antigen processing for major histocompatibility complex class I presentation. *Nat Immunol*. 2004; 5(7):670–677.
46. Reits E, et al. Peptide diffusion, protection, and degradation in nuclear and cytoplasmic compartments before antigen presentation by MHC class I. *Immunity*. 2003;18(1):97–108.
47. Botbol V, Scornik OA. Peptide intermediates in the degradation of cellular proteins. Bestatin permits their accumulation in mouse liver in vivo. *J Biol Chem*. 1983;258(3):1942–1949.
48. Reits E, et al. A major role for TPP1 in trimming proteasomal degradation products for MHC class I antigen presentation. *Immunity*. 2004;20(4):495–506.
49. Saric T, Beninga J, Graef CI, Akopian TN, Rock KL, Goldberg AL. Major histocompatibility complex class I-presented antigenic peptides are degraded in cytosolic extracts primarily by thimet oligopeptidase. *J Biol Chem*. 2001;276(39):36474–36481.
50. Shen L, Sigal LJ, Boes M, Rock KL. Important role of cathepsin S in generating peptides for TAP-independent MHC class I crosspresentation in vivo. *Immunity*. 2004;21(2):155–165.
51. Li Y, et al. Tumor-derived autophagosome vaccine: mechanism of cross-presentation and therapeutic efficacy. *Clin Cancer Res*. 2011;17(22):7047–7057.
52. Ma Y, et al. Anticancer chemotherapy-induced intratumoral recruitment and differentiation of antigen-presenting cells. *Immunity*. 2013; 38(4):729–741.
53. Falk K, Rotzschke O, Rammensee HG. Cellular peptide composition governed by major histocompatibility complex class I molecules. *Nature*. 1990; 348(6298):248–251.
54. Gitlitz BJ, et al. A pilot trial of tumor lysate-loaded dendritic cells for the treatment of metastatic renal cell carcinoma. *J Immunother*. 2003;26(5):412–419.
55. Jochem D, et al. Adjuvant autologous renal tumour cell vaccine and risk of tumour progression in patients with renal-cell carcinoma after radical nephrectomy: phase III, randomised controlled trial. *Lancet*. 2004;363(9409):594–599.
56. Lee WC, Wang HC, Hung CF, Huang PF, Lia CR, Chen MF. Vaccination of advanced hepatocellular carcinoma patients with tumor lysate-pulsed dendritic cells: a clinical trial. *J Immunother*. 2005; 28(5):496–504.
57. Schlom J. Therapeutic cancer vaccines: current status and moving forward. *J Natl Cancer Inst*. 2012; 104(8):599–613.
58. Kessler JH, et al. Antigen processing by nardilysin and thimet oligopeptidase generates cytotoxic T cell epitopes. *Nat Immunol*. 2011;12(1):45–53.
59. Silagi S. Control of pigment production in mouse melanoma cells in vitro. Evocation and maintenance. *The Journal of cell biology*. 1969;43(2):263–274.
60. Gamrekelashvili J, et al. Primary sterile necrotic cells fail to cross-prime CD8(+) T cells. *Oncoimmunology*. 2012;1(7):1017–1026.
61. Klein C, Bueler H, Mulligan RC. Comparative analysis of genetically modified dendritic cells and tumor cells as therapeutic cancer vaccines. *J Exp Med*. 2000;191(10):1699–1708.
62. Thomas MC, Gretten TF, Pardoll DM, Jaffee EM. Enhanced tumor protection by granulocyte-macrophage colony-stimulating factor expression at the site of an allogeneic vaccine. *Hum Gene Ther*. 1998; 9(6):835–843.
63. Mach N, Gillessen S, Wilson SB, Sheehan C, Mihm M, Dranoff G. Differences in dendritic cells stimulated in vivo by tumors engineered to secrete granulocyte-macrophage colony-stimulating factor or Flt3-ligand. *Cancer Res*. 2000;60(12):3239–3246.
64. Calogero S, et al. The lack of chromosomal protein Hmg1 does not disrupt cell growth but causes lethal hypoglycaemia in newborn mice. *Nat Genet*. 1999; 22(3):276–280.
65. Clarke SR, Barnnden M, Kurts C, Carbone FR, Miller JF, Heath WR. Characterization of the ovalbumin-specific TCR transgenic line OT-I: MHC elements for positive and negative selection. *Immunol Cell Biol*. 2000;78(2):110–117.
66. Hogquist KA, Jameson SC, Heath WR, Howard JL, Bevan MJ, Carbone FR. T cell receptor antagonist peptides induce positive selection. *Cell*. 1994; 76(1):17–27.
67. Gamrekelashvili J, et al. Necrotic tumor cell death in vivo impairs tumor-specific immune responses. *J Immunol*. 2007;178(3):1573–1580.
68. Oehen S, Brduscha-Riem K. Differentiation of naive CTL to effector and memory CTL: correlation of effector function with phenotype and cell division. *J Immunol*. 1998;161(10):5338–5346.
69. Wessel D, Flugge UI. A method for the quantitative recovery of protein in dilute solution in the presence of detergents and lipids. *Anal Biochem*. 1984; 138(1):141–143.
70. Keller A, Nesvizhskii AI, Kolker E, Aebersold R. Empirical statistical model to estimate the accuracy of peptide identifications made by MS/MS and database search. *Anal Chem*. 2002;74(20):5383–5392.
71. Nesvizhskii AI, Keller A, Kolker E, Aebersold R. A statistical model for identifying proteins by tandem mass spectrometry. *Anal Chem*. 2003; 75(17):4646–4658.